**1**

# Control of DNA Packaging by Block Catiomers for Systemic Gene Delivery System

*Kensuke Osada[1,2]*

[1] *National Institutes for Quantum and Radiological Science and Technology (QST), National Institute of Radiological Sciences (NIRS), Department of Molecular Imaging and Theranostics, 4-9-1 Anagawa, Inage-ku, Chiba 263-8555, Japan*

[2] *PRESTO, Japan Science and Technology Agency, 4-1-8 Honcho, Kawaguchi, Saitama 332-0012, Japan*

## 1.1 Introduction

DNA undergoes large volume transition from extended coil to compact state by polyion complexation with polycations for minimizing the contact surface area of the charge-neutralized polyplex from water [1–3]. The transition called DNA condensation is the essential mechanism of genomic DNA packaging and is the important process in preparing a nonviral gene delivery system [4–8]. The self-assembly formed from pDNA and block catiomers has been gaining attention as a potential systemic gene delivery system, in which the pDNA is condensed into a core by complexed with cationic block and the neutral blocks surround it as a shell to form a 100-nm-sized core–shell-structured polyplex micelle [9–12]. Polyplex micelles, launched from our group [13, 14], had been developed by the encouragement of the precedent development of polymeric micelles for drug delivery, which are currently under investigation of clinical trials [15, 16]. Originated from the firstly prepared polyplex micelles from PEG-*b*-P(Lys) [13, 17, 18], a variety of block catiomers or graft catiomers have been elaborated in order to improve the transfection efficiency by modulating parameters of their degree of polymerization (DP), grafting density for the case of graft catiomers, and varying mixing ratio with pDNA as described elsewhere in details [10, 17, 19, 20]. By these efforts, gene transfection efficiency has been remarkably promoted and a feasible formulation had proceeded to human clinical trial with local application [21, 22].

Nonetheless, development of polyplex micelles for systemic application has yet to be reached the level of clinical trial in spite of the structural analogy with polymeric micelles for drug delivery. This is mainly ascribed to the limited bioavailability of pDNA in active form at the final targeted nucleus; particularly, its instability in bloodstream precludes the secure delivery. To this end, the key issue that should be addressed is the packaging of pDNA into polyplex micelles because it regulates the basic character of polyplex micelles such as

size, surface potential, stability, shape, and PEG crowding and thereby their biological performances such as blood circulation capacity, protection from nuclease attack, efficiencies of extravasation and migration into tissue, cellular entry efficiency, and transcription efficiency, all of which affect the ultimate gene expression efficiency. For achieving proper packaging, it is imperative to know the character of pDNA as a molecule and the principle mechanism of polyplex micelle formation so as to freely handle the structure. Moreover, it is necessary to know the suitable structure and the required functionalities to accommodate each step of delivery process. These processes should clearly point out the demanding issues for entirely managing the systemic gene delivery, which ultimately lead to a proper molecular design in structure and functionality to prepare polyplex micelles for achieving systemic gene therapy.

In this context, this review first focuses on the packaging of pDNA by block catiomers as the primal subject. Then, the required property and functionality for managing each of the delivery process are focused from intravenous (IV) injection to the last process of transcription. Finally, rational design criteria of block catiomers for systemic gene delivery are outlined.

## 1.2 Packaging of pDNA by Block Catiomers

It is important to first recognize the molecular character of pDNA for the sake of elucidating the mechanism of pDNA packaging. pDNA is a large molecule comprising typically a few kbp, which correspond to millions in molecular weight and a few micrometers in contour length, and has supercoiled closed circular form. DNA behaves as a semiflexible chain in solution with persistence length of 50 nm. Then, it is complexed with a large number of block catiomers for compensating the negative charges of pDNA, e.g. 200 block catiomers are required to compensate negative charges of pDNA of 5000 bp when block catiomers with 50 positive charges in their cationic segment are used. The formed polyplex micelles consist of single pDNA, wherein the concept of CAC is not defined as opposed to the polymeric micelles prepared from amphiphilic block copolymers, which are formed by association of multimolecules. Note that the single pDNA packaging is ensured as long as conducting the complexation at a diluted condition, which allows the accomplishment of the PEG shell formation before the collision of complexed pDNA to associate with neighboring complexed pDNA molecule due to translational motion. Otherwise, the secondary association occurs when the polyplex collision takes place faster than the formation of PEG shell, which is evidenced in the network-like complex formation by conducting the complexation exceeding the overlapping concentration of pDNA strands [23]. Polyplex micelles are characterized as approximately 100 nm particles by dynamic light scattering (DLS) and neutral zeta-potential value due to the charge-shielding effect by the PEG shell. When considering packaging of pDNA into polyplex micelles with respect to the aforementioned character of pDNA, several fundamental questions should rise: how the long pDNA changes its conformation within the characteristic topology and how

**Figure 1.1** Packaging of pDNA within polyplex micelles by PEG$_{12k}$-P(Lys)$_{70}$ block catiomers observed by TEM. Various shapes are observed: (a) rod shape, (b) toroid shape, and (c) globular shape.
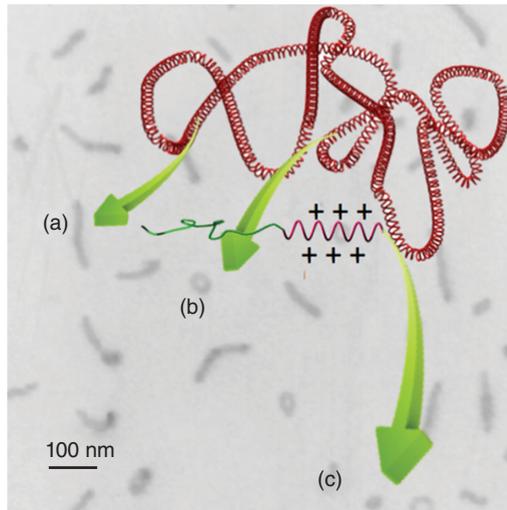


DNA accommodates its stiffness. To these questions, transmission electron microscopic (TEM) or AFM observations revealed that pDNA undergoes a variety of packaging to form structural polymorphism [24–31] such as rod shape, doughnut-like shape (toroid), and globular shape (Figure 1.1). This is actually intriguing with respect to the driving force of the DNA condensation because globular shape is the most expected shape for minimizing the surface area. The next section deals with the subject of pDNA packaging to address this question focusing on the rod shape and globular shape.

### 1.2.1 Rod-Shaped Packaging of pDNA

The rod shape is the most frequently observed shape among structural polymorphism. A specific folding scheme of pDNA was found from the study based on PEG-*b*-poly(L-lysine) [PEG-*b*-P(Lys)] polyplex micelles, named "quantized folding scheme." pDNA is folded by *n*-times ($f_n$) to form a rod shape consisting of $2(n+1)$ numbers of double-stranded DNA packed as a bundle in the orthogonal cross section (Figure 1.2b). Accordingly, the length is regulated to multiple of $1/[2(n+1)]$ of pDNA contour length as found in the discrete rod length distribution measured from TEM images (Figure 1.2a) [32]. This folding scheme has been observed in various polyplex micelles irrespective of the species of hydrophilic block and cationic block [30, 33] as well as the length of pDNAs; thus, it takes place independent of DNA sequences [34]. Another intriguing scheme is the relevancy with DNA rigidity; DNA is folded back at the rod ends, which is actually unacceptable assuming the persistence length of the double-stranded DNA (50 nm). However, this is made possible by local dissociation of double-stranded structure at the rod ends. The flexible nature of single-stranded DNA with persistence length of a few nanometers or less permits DNA to fold back. S1 nuclease, a single-stranded DNA-specific nuclease, could detect the occurrence of the double-stranded DNA dissociation,
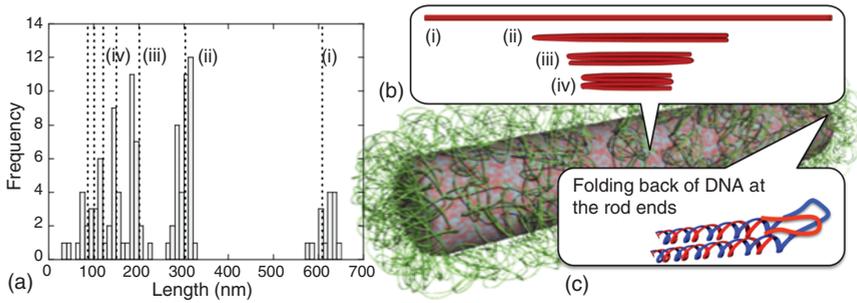
**Figure 1.2** Quantized folding scheme of pDNA to form bundled structure within polyplex micelles. (a) Rod length distribution measured from TEM images. (b) DNA is folded to bundled rod within polyplex micelles. Folded pDNA (i)–(iv) in (b) corresponds to the rod lengths in (a). (c) Double-stranded structure of DNA at the rod ends is locally dissociated to single strand for folding back.

presenting a specific fragmentation pattern with lengths exactly corresponded to the multiples of the rod lengths [28, 32, 34].

The rod length, determined by $f_n$ of pDNA, was changed by DP in P(Lys) block. The rod length shifted to short with increasing P(Lys) DP; major $f_n$ was 1–5, 2–8, and 3–9 for polyplex micelles prepared from $PEG_{12k}$-$b$-P(Lys) with P(Lys) DP 19, 39, and 70, respectively [35]. This P(Lys) DP dependence is mechanistically accounted based on the PEG contribution. A quantitative analysis of the PEG crowding of polyplex micelles allowed for depicting the rod shape by the balances of free energies for DNA compaction ($dF_{compaction,DNA} = Gl\,dl - dE_{surface}$) and free energies for PEG repulsion ($dF_{anti\text{-}compaction,PEG} = \Pi(dV_{occ,PEG}) - T(dS_{conf,PEG})$). Here, $G$, $l$, $E_{surface}$, $\Pi$, $V_{occ,PEG}$, $T$, and $S_{conf,PEG}$ represent modulus of rigidity of bundled DNA core, rod length, surface energy developed on the core, PEG osmotic pressure, number-average occupied volume of PEG, temperature, and conformational entropy of PEG, respectively. Briefly, polyplex micelles prepared from lower P(Lys) DP retain more number of PEG in the shell because the associating number of block catiomer is inversely proportional to P(Lys) DP. Thus, those polyplex micelles are elongated by the increased PEG steric repulsion. The long rod structure costs higher interfacial free energy than the shorter rod; thus, the higher PEG crowding than the shorter rod balances it. Eventually, the long rod shape has the higher PEG crowding for accommodating the energetic balance. The consistent relevancy is observed between the rod length and analyzed PEG crowding. The $PEG_{12k}$-$b$-P(Lys)$_{70}$ polyplex micelles showing shorter rod length were analyzed to have so-called mushroom conformation from the estimated reduced tethering density (RTD) value of 2.6, whereas the $PEG_{12k}$-$b$-P(Lys)$_{20}$ showing longer rod length was analyzed to have upward squeezed conformation from the RTD value of 5.2 [35]. The cryo-TEM observation confirmed the consistent PEG height with those analyzed PEG conformation [35].

The energetic description in the rod shape is further examined by the investigation using PEG cleavable polyplex micelles prepared from $PEG_{12k}$-acetal-P(Lys)$_{19}$ block copolymers [36]. Upon incubating the polyplex micelles in acidic milieu

for releasing PEG blocks from the polyplex core, the originally formed rod shape had changed to globular shape, indicating that the presence of PEG sustained the rod shape from being globular shape. This study concomitantly revealed the contribution of rigidity of the bundled DNA in the rod shape. The rod shape maintained the lengths unchanged even when PEG had been continuously removed out from polyplex micelles representing the contribution of the bundled DNA rigidity to sustain the rod shape. The rod shapes had, however, collapsed into globular shapes when the synergistic contributions of PEG and DNA rigidity could not endure the request of DNA condensation.

### 1.2.2 Rod Shape or Globular Shape

It is found that pDNA is condensed into a globular shape by complexing with homo-catiomers [23, 37], which is actually the most expected shape following the request of DNA condensation. This fact indicates that the presence of PEG interferes the condensation into the globular shape, suggesting a possibility that the extent of PEG interference may regulate the condensation into rod shape or globular shape. This view is examined by modulating the PEG crowding on polyplex micelles prepared from PEG-*b*-P(Lys) block catiomers through changing the number of associated PEG on complexed pDNA attainable by changing DP of P(Lys) block or changing the PEG volume by changing the molecular weights of PEG block. Consequently, it was found that the PEG crowding covering pDNA in a pre-condensed state before undergoing condensation regulated the packaging pathways to form either structure. The rod shape was preferentially formed when the tethered PEG chains in a pre-condensed state were dense enough for overlapping one another, whereas the globular shape was preferentially formed when they were not overlapped [23]. In the $PEG_{12k}$-*b*-P(Lys) block catiomers, the globular shape becomes predominant when P(Lys) DP was higher than 100. It should be noted that DNA double-stranded structure is impaired to dissociation in the globular shape as evidenced by the S1 nuclease assay so that DNA can accommodate the rigidity issue [23].

These mechanistic studies have provided a general scheme to understand structures of polyplex micelles prepared from various block or graft catiomers. For example, change in rod length was observed for polyplex micelles prepared form PEG-*g*-cysteine-P(Lys)$_{30}$ with fixed P(Lys) DP and varied PEG molecular weight [29]. This can be interpreted that the increased PEG crowding on polyplex micelles by the increased PEG molecular weight eventually elongated the rod length. The rod-shaped polyplex micelles prepared from poly[2-(methacryloyloxy)ethylphosphorylcholine]$_{30}$-*b*-poly(dimethylaminoethyl methacrylate), PMPC$_{30}$-*b*-PDMAEMA, decreased their rod length by increasing DP of PDMAEMA segment from 10 to 40 [24]. This trend is consistent with the increase in P(Lys) DP in the PEG-P(Lys) polyplex micelles and is understood that the increased DP of PDMAEMA segment decreases the number of associating PMPC chains and results in a decrease in the PMPC crowding, thereby permitting polyplex core to take shorter rod. The polyplex micelles changed the predominant shape from rods to globules by further increasing DP of PDMAEMA up to 60, which is again the same trend with the observations

for PEG-P(Lys) polyplex micelles. Globular shape was also found in the polyplex micelles formed from $PEG_{3k}$-*b*-$DMAEMA_{100}$ [38] and $PEG_{2k}$-*b*-$DMAEMA_{37}$ [39]. The formation of these globular shapes are understood by the fact that the decreased number of PMPC chains or lowered PEG molecular weight permitted pDNA to undergo globular collapsing instead of rod folding. The variation of structures was also found by modulating solvent polarity for complexation. Polyplex micelles of $PEG_{10k}$-*b*-polyphosphoramidate (PPA) formed long rod shapes by preparing in pure water. This was changed to shorter rod shape and ultimately changed to globular shape by increasing DMF fraction in the DMF/water cosolvent [40]. This could be presumed that the change of solvent polarity changed the energetic balance for the condensation and anti-condensation, leading to such structural change.

In this way, these studies have provided potential answers to the fundamental questions concerning the conformational change of DNA strands and the rigidity of DNA upon condensation and also the rod-shaped formation instead of the globular shape.

## 1.3 Polyplex Micelles as a Systemic Gene Delivery System

After understanding the basic structural characters, it is important to know the suitable structure and the required functionalities to accommodate each step of delivery process so that one could identify demanding issues for entirely managing systemic gene delivery. This section focuses such issues starting from a subject of stable encapsulation as the basic requirements for circulation, cellular entry, endosome escape, nuclear translocation, and ultimate transfection efficiency.

### 1.3.1 Stable Encapsulation of pDNA Within Polyplex Micelles for Systemic Delivery

Polyplex micelles need to overcome various biological barriers as depicted in Figure 1.3, whereby they confront a variety of biological components that preclude their systemic delivery such as nucleases, negative-charged substances to cause disassembly of polyplex through polyion exchange reaction, and inherent biological defense system. This section describes the required structure and functionality against these obstacles.

Nuclease attack gives fatal impact for gene delivery because pDNA impairs the ability of gene expression even permitting one site cleavage along the long DNA strands. It is acknowledged that the complexed pDNA attains tolerability against nuclease attack and the PEG shell coverage further improves tolerability [12, 14, 18, 34]. However, pDNA was still ultimately digested even within polyplex micelles with elevated PEG crowding during systemic circulation [35]. Thus, a strategy to physically block the access of nucleases was considered. It is thought that such polyplex micelles may be prepared from block copolymers retaining hydrophobic segment serving for blocking layer; however, the
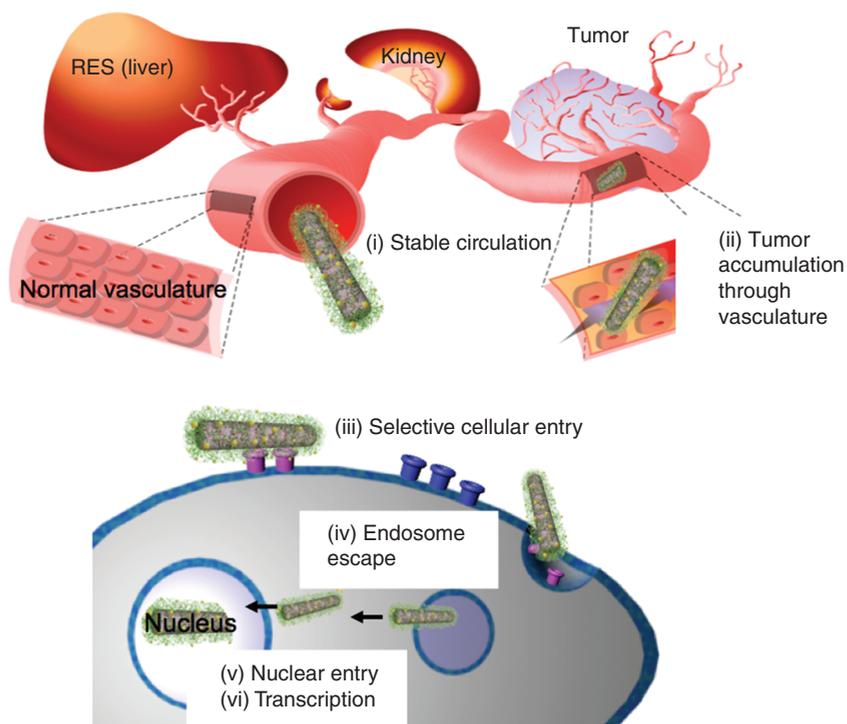
**Figure 1.3** Schematic illustration of systemic gene delivery processes.

hydrophobic segment may spontaneously cause interpolymer association before complexation with pDNA, giving rise to interference in the smooth polyion complexation. This problem is smartly solved by use of thermoresponsive polymers, which behave as a hydrophilic chain in the solution below the lower critical solution temperature (LCST) while it behave as a hydrophobic chain in the solution above the LCST. Thus, a triblock copolymer consisting of hydrophilic poly(2-ethyl-2-oxazoline), thermoresponsible poly-(2-*n*-propyl-2-oxazoline) (PnPrOx), and cationic P(Lys) was designed noticing its lower LCST(25 °C) than the body temperature. A two-step procedure, mixing the triblock copolymers with pDNA below the LCST of PnPrOx followed by incubation above the LCST (37 °C), allowed for collapsing of the PnPrOx segment positioning in the middle layer of polyplex micelles [30]. The polyplex micelles exhibited significant tolerance against nuclease attacks over the control polyplex micelles without the protective layer, presenting great utility of this strategy for preventing the nuclease access. Such double-protective-layered polyplex micelles were also prepared from diblock catiomers but from a set of diblock catiomers each having hydrophilic block and thermoresponsive block. These were prepared by complexing pDNA with a mixed block catiomers of PEG-*b*-poly{*N*′-[*N*-(2-aminoethyl)-2-aminoethyl]aspartamide} {PEG-*b*-P[Asp(DET)]} and poly(*N*-isopropylacrylamide)-*b*-P(Asp(DET)) (PNIPAM-*b*-P(Asp(DET)) at

room temperature, which is below the LCST of PNIPAM, for the formation of polyplex micelles with hydrophilic shell of PEG and PNIPAM, followed by incubation at 37 °C for collapsing the PNIPAM segment to prepare hydrophobic palisade. The polyplex micelles also exhibited significant improvement in nuclease tolerability compared with those without hydrophobic palisade [31].

Association with negatively charged substances is another critical factor for precluding the bioavailability of polyplex micelles because it causes disintegration of polyplex micelles through polyion exchange reaction. Note that this is a common problem in most of the nucleic acid delivery systems prepared by electrostatic assembly [41, 42]. Typically, glycosaminoglycans (GAGs), negatively charged polysaccharides, including chondroitin sulfate (HS) and heparan sulfate (HS), are addressed as such substances. These molecules are abundantly presenting in the cell membrane, including vascular endothelial cells and blood cells, and in the glomerular basement membrane in kidney; therefore, polyplex micelles inevitably encounter them during the delivery process, particularly during cellular entry and blood circulation. In this view, strategies of stabilization are imperative in addition to the inherent electrostatic interaction, although overstabilization impairs the transcription process. This trade-off can be addressed by core cross-linking with redox-responsive disulfide linkage because it allows for maintaining the linkage in extracellular entity including bloodstream, while it is cleaved in the intracellular reductive environment [25, 43–45]. Photocleavable cross-linkers and pH-responsive cross-linkers are also feasible reversible cross-linkers to manage the trade-off. Phenylboronic acids (PBA) are a recently highlighted cross-linker, worked by dual stimuli of pH and ATP concentration [46]. An installation of hydrophobic group into the core compartment is another effective strategy to prevent disintegration through its coagulation force, although it has no reversibility [47–49]. DNA intercalators, such as acridine, were also considered to prevent the dissociation, although the no reversibility and the inherent carcinogenic property remain as a concern [50]. The aforementioned hydrophobic barrier compartment can also improve the stability due to its blocking capacity against the access of GAGs to the polyplex core [30, 31]. Polyplex micelles modified with these strategies eventually promote longevity in blood circulation as well as later-described cellular uptake efficiency.

A property to prevent adsorption of biological compounds present in blood is important for ensuring prolonged blood circulation aside of the stabilization. Nonspecific interaction causes the formation of aggregates, which readily results in embolization of capillary. Furthermore, adsorption of serum proteins triggers the elimination by mononuclear phagocyte system (MPS) [51]. It is widely acknowledged that PEGylation affords this property onto nanocarriers [11, 12, 52–54]. The significance of the PEG shell is indeed visualized by the *in situ* observation using the intravital real-time CLSM (IVRTCLSM) [55]. Polyplexes prepared from non-PEG catiomers immediately caused the formation of distinct aggregates after intravenous injection, whereas their PEGylated micelle formulation was observed to circulate without such aggregate formation. To prevent the adsorption of serum proteins, it is important to consider PEG crowding of polyplex micelles because it determines the extent of serum

protein adsorption. It is reported that inhibition of the protein adsorption on PEG-modified surface started when PEG chains were crowded for overlapping with neighboring chains and maximized when the overlapped PEG chains were substantially crowded ($\langle L \rangle / 2R_g < 0.48$; $L$ indicates distance between tethering PEG sites) [51]. In this regard, PEG crowding of polyplex micelles prepared from $PEG_{12k}$-P(Lys) block catiomers was evaluated, giving $\langle L \rangle / 2R_g = 0.39$, 0.47, and 0.55 for polyplex micelles of $P(Lys)_{19}$, $P(Lys)_{39}$, and $P(Lys)_{70}$, respectively [35]. The PEG crowding suggested that polyplex micelles with $P(Lys)_{19}$ and $P(Lys)_{39}$ may have higher chance to escape the elimination mode by MPS, whereas those with $P(Lys)_{70}$ may be captured. The evaluation using IVRTCLSM consistently proved the projection because the blood circulation profiles were improved in the following order: $P(Lys)_{70} < P(Lys)_{39} < P(Lys)_{19}$ [35]. Notably, the profiles showed that a certain fraction had been eliminated from the bloodstream at the early circulating stage for polyplex micelles of $P(Lys)_{70}$. It should be further noted that polyplex micelles prepared from $PEG_{20k}$-P(Asp(DET))$_{60}$-Chole were analyzed to have much high PEG crowding with scalable brush conformation and exhibited a profile suggesting successful escape from the early elimination mode [48]. These observations demonstrate that the PEGylation can indeed serve for prolonging the blood circulation, but the crowding is essential for escaping the early elimination mode.

In addition, a crucial impact of shear stress was recently indicated in the capacity of blood circulation. It was demonstrated that the shear stress removed block catiomers from polyplex micelles when they were exposed at magnitudes in the bloodstream resulted in structural deterioration, which eventually led to accelerated degradation by nucleases. Instead, installation of the core cross-linking prevented the structural deterioration and remarkably improved the blood circulation profile [56]. Thus, it is reasonable to assume that the stabilization by either means of cross-linking, hydrophobic moieties or intercalators, can improve the tolerability against shear stress and thereby improve the blood circulation [25, 47, 50, 57, 58].

### 1.3.2 Polyplex Micelles for Efficient Cellular Entry

Polyplex micelles are intrinsically unfavorable for cellular entry because the presence of PEG shell prevents association with cell surface; particularly, an attempt to elevate PEG crowding for improved shielding further impairs their interaction with cells. Moreover, as opposed to positively charged non-PEG polyplexes, polyplex micelles with neutral zeta-potential do not have strong interaction with negatively charged cells. Furthermore, GAGs on cellular membrane cause destabilization of polyplexes. Thus, the installation of stabilizing functionality as described in Section 1.3.1 can promote their cellular uptake efficiency [25, 47–49, 59]. Ligand molecules can also promote the cellular uptake efficiency for which transferrin [11], peptides such as cRGD [52] or peptides for EGFR [60], sugars, aptamers, and antibodies [11, 61–63] are often used. In the choice of ligands, it is important to consider not only the efficiency but also the specificity to distinguish the targeted cells from nontargeted cells in order for avoiding false delivery. Also, the ligand molecules should not compromise the stealth

effect of the carriers. In this sense, cell-penetrating peptides (CPP) [64–68] may not be suitable for systemic application due to their limited cell specificity and their positive charges cause nonspecific interaction with biological molecules, although the strong potency to promote cellular entry is attractive. After choice of appropriate ligands, it is important to consider the ligand density on polyplex micelles for obtaining maximized efficacy. The low ligand density may not suffice to ensure the multivalent binding with their receptors, whereas the high density may impair the stealth character of the carriers. Moreover, the strong multivalent binding with receptors may not allow the captured polyplex micelles release to the other side, resulting in the decreased efficiency of transcytosis [69]. It is also important to consider the mobility of the attached ligand molecules on the polyplex micelles for providing a chance to bind with receptors [70]. PEG cleavage is an interesting strategy to tackle the so-called PEG dilemma. Disulfide bond was installed between PEG and catiomer to expect PEG cleavage at the extracellular space [71–75]. This strategy could be effective in local applications although the nonspecificity may be not suite for systemic application. In this respect, peptides susceptible to matrix metalloproteinase (MMP), presenting rich in tumor, may be useful [76, 77].

In addition, it is addressed that the shape and size are the parameters to determine cellular uptake [78]; e.g. inhibited cellular uptake was observed for filamentous nanoparticles [79–81]. Nonetheless, it is still controversial because different nanoparticles with different surface properties are used in order to change their sizes and shapes. To this issue, polyplex micelles of $PEG_{21k}$-P(Lys)(SH) revealed a significant effect of rod length on cellular uptake based on their capacity to change the rod length but maintaining their surface properties including PEG crowding and zeta-potential. Note that the polyplex micelles were installed with disulfide cross-linking to address the GAG-mediated destabilization upon cellular entry. This study uncovers the critical rod length of 200 nm for efficient uptake [59]. This was reasonably explained by the upper limit sizes of endocytotic vesicles, which were evaluated as 5 μm [82], 200 nm [83, 84], 80 nm [85], and 90 nm [86] for macropinocytosis, clathrin-dependent, caveolae-dependent, and clathrin/caveolae-independent endocytosis, respectively. Thus, polyplex micelles with rod length fractions below 200 nm can be taken up by any of these four endocytotic pathways, whereas that rod length fraction above 200 nm can be taken up only by macropinocytosis. The rod length limitation was observed in various cell lines including HeLa, BxPC3 cells, and HUVECs in the examined PEG-P(Lys) polyplex micelles as well as in other polyplex micelles prepared from PMPC-*b*-PDMAEMA block catiomers against A549 cells [24] and PEG-*b*-PPA against HEK 293 cells [40]. Importantly, the modifications of cRGD peptide on PEG-*b*-P(Lys) polyplex micelles could remarkably increase the cellular uptake efficiency for the polyplex micelles, which satisfied the rod length limitation, i.e. PEG-*b*-P(Lys)$_{42}$ and PEG-*b*-P(Lys)$_{69}$, but not for polyplex micelles with rod length above the 200 nm, i.e. PEG-*b*-P(Lys)$_{20}$, indicating the significance of rod length limitation.

### 1.3.3 Polyplex Micelles for Safe Endosome Escape

Endosome escape is addressed as a major barrier for gene delivery; otherwise, the cargo pDNA is subjected to digestion in the later fused lysosomes or recycling to the cell surface. Several polycations have been proposed to promote the endosome escape, including PEI [11, 52, 87–89], poly(histidine) [90–93] poly(amidoamine) dendrimers [94–96], or N-substituted polyaspartamide [97] including P(Asp(DET)) [98]. It is interesting to notice that these polycations commonly retain amine groups with low $pK_a$ around 5.5–7.4 within the structures, which can promote their number of cationic charges in endosomal pH 5.5. The change in the degree of protonation between pH 7.4 and 5.5, namely buffering capacity, is thought to be essential for exerting endosome escape by so-called proton sponge effect relying on the increase of endosomal osmotic pressure [87, 89], or by direct membrane disruption relying on the protonated polycations [17, 99–101]. The latter mechanism has recently been recognized as a more plausible account for the endosome escape functionality by those amines. Investigations to gain insight into the mechanism of the endosome escape were demonstrated by focusing on the aminoethylene unit, which is a repeating unit of linear PEI. A series of polyaspartamides bearing 1–4 repeating number ($R$) of the aminoethylene unit in their side chain was prepared by aminolysis reaction with poly(β-benzyl-L-aspartate) (PBLA), which allowed for introducing amine compounds [102] of ethylene diamine (EDA) for $R1$ (=PAsp(EDA)), diethylenetriamine (DET) for $R2$ (=P(Asp(DET))), triethylenetetramine (TET) for $R3$ (=PAsp(TET)), and tetraethylenepentamine (TEP) for $R4$ (=PAsp(TEP)) to the polymer chain [97]. Interestingly, their buffering capacity (0.06, 0.31, 0.10, and 0.17 for $R1$, $R2$, $R3$, and $R4$, respectively) did not completely correlate with the order of their observed endosome escapability: $R4 > R2 > R3 > R1$. Instead, their endosome escapability was correlated with the order of hemolytic activity: $R4 > R2 > R3 > R1$ [97]. This observation supported the mechanism based on the membrane disruption by polycations being more plausible rather than the mechanism based on the proton-sponge effect. More interestingly, an odd–even effect was observed in their endosome escapability. Polymers of $R1$ and $R3$ did not show pH-depending hemolysis activity but polymers of $R2$ and $R4$ showed significant hemolysis activity only at pH 5.5, eventually the latter group elicited promoted endosome escapability. In the similar line, a block catiomer containing tetraethylenepentamine units [103] or 4 aminoethylene units of tetraethylenepentamine (TEPA) in the side chain [75] was prepared and efficient endosome escapability was demonstrated. Of note, PEI consists of aminoethylene units in the structure; however, the augmented repeating number induces high membrane destabilization already at pH 7.4, thereby causing strong cytotoxicity. In this regard, deconcentration of aminoethylene, such as pendant to the main chain, may be a good strategy to exert endosome-selective membrane destabilization but not for other membranes, such as cellular, mitochondrial, or nuclear membranes, so as to minimize cytotoxicity.

Although the tempting endosome escape capacity of those polycations, it appears that the presence of PEG shell in their polyplex micelles hampers direct

association of those polycations with endosome membrane, impairing the implementation of the membrane disruption. Study using polyplex micelles prepared from PEG-*b*-P(Asp(DET))-Chole demonstrated an intriguing mechanism for it. Polyplex micelles released a fraction of polymers in the pH 5.5 so as to compensate the overcharge caused by the promoted protonation of the P(Asp(DET)) [47]. The released polymers are facilitated to associate with endosome membrane by the attached cholesteryl group at the polymer end [49]. Note that the polymer with single protonated state at pH 7.4 shows moderate membrane destabilization; however, that with promoted protonation state exerts marked membrane destabilization [98]. It should be noted that polyplex micelles lack block catiomers to sufficiently compensate pDNA charges in the neutral cytoplasmic environment because the polymers have now recovered the initial mono-protonated state and polyplex micelles have released a fraction of polymers in the previous endosome. This circumstance let the condensed pDNA loosen, facilitating the subsequent transcription process. In this way, the amine groups with lower $pK_a$ values elicit not only endosome escape functionality but also transformation into transcription-favorable form. Noteworthy, this molecular mechanism is applicable for any catiomers containing protonatable amino groups in the endosomal acidic condition, submitting a potential explanation for facilitated endosome escape by catiomers with buffering capacity, including PEI.

The attached ligand could also contribute for facilitating the endosome escape because of its capacity to modulate the intracellular fate. It is reported that some peptides containing amphipathic sequences change membrane integrity so as to enhance intracellular delivery by destabilizing the endosome membrane [63, 94, 104, 105]. In addition, polyplex micelles prepared from PEG-*b*-P(Lys) attached with cRGD peptides are observed for accumulation at perinuclear region in the early stage even though the P(Lys) does not retain specific endosome escape functionality [106]. This observation suggested that the cRGD might circumvent endosome entrapment by steering an alternative pathway. The same trend was observed for cross-linked polyplex micelles of cRGD-PEG-P(Lys) for siRNA delivery [107].

Physical stimuli, such as light, are potential tool for facilitating endosome escape, known as photochemical internalization (PCI). This is mediated by reactive oxygen species (ROS) produced by photosensitizers upon photoirradiation [108–110]. However, the photosensitizers tend to form aggregates in aqueous solution and limit the ability of ROS production. This problem was solved by the development of phthalocyanine-loaded dendrimers (DPc), incorporating a photosensitizer in the focal core of the dendrimers [111, 112]. The DPc was attached with 32 carboxyl groups on the periphery so that it could polyion-complex with positively charged polyplexes. The polyplexes demonstrated a remarkable photoinduced endosome escape functionality [113]. Further, the DPc was applied to polyplex micelles wherein a specialized compartment was prepared for DPc loading within polyplex micelles, exhibited significant light-accelerated endosome escape functionality [114], opening door to use PCI in systemic application, which is described in Section 1.4.

### 1.3.4 Polyplex Micelles for Nuclear Translocation

pDNA needs to access nucleus for exerting gene expression. The chance is only during the mitosis when the nuclear envelope transiently disappears and the non-viral gene delivery relies on this pathway, as evidenced in cell-cycle-dependent gene expression profile [106, 115, 116]. Otherwise, nuclear pore complex (NPC) is considered the only way for nuclear entry. It is reported that the NPC allows passive diffusion of small molecules up to 9 nm in diameter or active transport of larger molecules (~26 nm) by attaching nuclear localization sequences (NLS) [117]. It is reported that gold nanoparticles with diameter close to 39 nm coated with NLS and importin α and importin β were translocated to nucleus [118]. However, whether gene carriers attached with NLS really cross the NPC still remains controversial due to the lack of assured technique to prove it [119]. It should be noted that packaging of pDNA into such small is technically difficult due to its large molecular weight and the intrinsic rigidity. Gene expression in nondividing cells is the future challenge; however, once it permits, the potential of gene therapy expands versatile cells and wide range of diseases. Of note, even the nuclear entry through NPC cannot be made, the NLS conjugation may be practically feasible in dividing cells because its conjugation can facilitate accumulation at perinuclear region, leading to an increase in the probability of the nuclear entry when it opens.

### 1.3.5 Polyplex Micelles for Efficient Transcription

Transcription is the last important step after the long journey of gene delivery for achieving gene expression. The process involves assembly of several subunits of transcription factors on DNA together with RNA polymerase to complete the formation of transcription machinery and following its sliding along DNA strands to produce mRNA. This process appears unfavorable in the packaged pDNA [120–126] and further by PEG shielding. The investigation in the cell-free system, however, indicated that transcription underwent for pDNA in the PEG-P(Lys)-based polyplex micelles, but the efficiency was highly dependent on PEG molecular weight and P(Lys) DP [34]. Note that immediate dissociation of polyplex micelles before transcription was unlikely to occur since polyplex micelles have been confirmed to be stable in physiological buffer [34] and in 90% serum [35], suggesting that pDNA in polyplex has certain dynamic mobility sufficient for permitting transcription. The critical PEG crowding for inhibiting transcription was suggested from the study using polyplex micelles having similar folding number of pDNA but have shells of different PEG crowding, prepared from PEG-*b*-P(Lys) with fixed P(Lys) DP around 70 and varied PEG molecular weight (12k–42k). The appreciable transcription was observed in polyplex micelles with lower PEG molecular weight of 12 and 21 k, while it was impaired in the polyplex micelles with 30k and 42k [23]. It is interesting to note that the PEG crowding analysis indicated that the crowding of the former group was of higher level than the critical crowding to exhibit prevention of protein

adsorption ($\langle L \rangle / 2R_\mathrm{g} < 0.47$) [51], while that of the latter group was analyzed to be the level of permitting the protein adsorption ($\langle L \rangle / 2R_\mathrm{g}$ for those polyplex micelles with PEG 12, 21, 30, and 42 k was analyzed to be 0.68, 0.47, 0.38 and 0.33, respectively). Transcription was also affected by the packaging structure of pDNA, which was examined by polyplex micelles with fixed PEG $M_\mathrm{w}$ 12 k while varying P(Lys) DP from 20 to 145. The cell-free evaluation showed that the transcription efficiency significantly decreased with increase an in P(Lys) DP. Noteworthy, this trend was well correlated with the increased fractions of the globule-shaped packaging, suggesting that globular shape was unfavorable for transcription.

## 1.4 Design Criteria of Block Catiomers Toward Systemic Gene Therapy

The reviews on each step of gene delivery allowed us for noticing several crucial requirements for accommodating entire systemic delivery. The most critical requirement should be highlighting the rod length limitation for cellular uptake, which involves several trade-off issues. The attempt to augment PEG crowding for improving circulation property leads to elongation of the rod length [35], which results in impairment of cellular uptake capability and thus transfection efficiency [40]. Further, the transcription efficiency preferentially undergoes for polyplex micelles with longer rod length but those are unfavorable for cellular uptake. This trade-off issue was clearly evident in polyplex micelles of cRGD-PEG$_{21\mathrm{k}}$-*b*-P(Lys)(SH) with P(Lys) DP 20 and 70. The former polyplex micelles having longer rod length with their fraction mostly above 200 nm showed better transcription capability, higher PEG crowding, and better blood circulation profile compared with those of the latter one; however, they resulted in limited transfection efficiency *in vitro* as well as *in vivo* after systemic application and failed for achieving anti-tumor efficacy [59]. In contrast, the latter polyplex micelles having their rod length fraction below 200 nm showed appreciated transfection efficiency and exhibited significant systemic anti-tumor efficacy against subcutaneous pancreatic tumor model by the antiangiogenic approach using fms-like kinase-1 (sFlt-1), in spite of their inferior transcription capability and blood circulation profile as compared with the former polyplex micelles. This consequence indicated that the regulation of the rod length is the primal requirement even compromising blood circulation capacity and transcription efficiency. Therefore, a strategy derived is to augment the transfection efficiency for obtaining maximized gene expression from the successfully delivered pDNA. The major strategy is use of catiomers that elicits the endosome escape functionality and conjugation of ligand molecules. Thus, polyplex micelles prepared from PEI and coupling with ligands, such as transferrin [11], RGD [52], or EGFR specific peptides [60], have been proposed and successful systemic tumor gene transfection was reported. Contrast to PEI, which remains a toxic concern, a catiomer of P(Asp(DET)) is appealing because of the significant endosome escape capacity [98] as well as the appreciated safety profile relying on the unique

self-degradation profile in the physiological condition [127]. Several attempts have been made to utilize this potential catiomer in systemic application. Taking the advanced capacity of homo P(Asp(DET)) to promote endosome escape and cellular uptake efficiency, block-/homo-integrated (B/H)) polyplex micelles were developed and succeeded to demonstrate antitumor efficacy not only in local applications [128, 129] but also in systemic application [37]. Augmentation of stability was also a feasible strategy to promote PEG-*b*-P(Asp(DET)) for systemic application. The stabilized PNIPAM$_{5k}$-P(Asp(DET))/PEG$_{12k}$-P(Asp(DET)) polyplex micelles by the hydrophobic barrier compartment addressed the nuclease tolerability, cellular uptake, and endosome escape and achieved promotion in transfection efficiency. With remarkably improved blood circulation capacity, the polyplex micelles demonstrated antitumor efficacy by the antiangiogenic therapy against H22 tumor-bearing mice [31]. The prominent effect of PCI to promote endosome escape was attempted to use for systemic application. To this end, a triblock catiomer of PEG-*b*-P(Asp(DET))-*b*-P(Lys) was designed to prepare compartmentalized polyplex micelles for loading DPc. Here, selective complexation of each cationic block played a significant role. The P(Lys) block specifically complexed with pDNA to form a core compartment and the P(Asp(DET)) block specifically complexed with DPc [130] to form a middle compartment under the PEG shell. The compartmentalized polyplex micelles addressed several critical issues requesting for PCI in systemic application: DPc prevents aggregation of photosensitizers to cause self-quenching [111–113]; delivery of DPc and pDNA in one system ensures their colocalization at endosomes; and separated packaging of DPc and pDNA in each compartment minimizes the photochemical damage to the cargo pDNA. The gene expression efficiency was promoted to 2 order of magnitude higher by photoirradiation and exhibited light-induced *in vivo* gene transfer in subcutaneous HeLa tumor as well as HCT 116 tumor following systemic administration, representing the first success in the PCI-mediated systemic gene transfection [114]. Noteworthy, the system exhibited no gene transfection without photoirradiation, appealing its safety profile. The aforementioned polyplex micelles prepared from cRGD-PEG$_{21k}$-*b*-P(Lys)$_{69}$(SH) block catiomers exerted transfection efficiency as high as ExGen 500 (linear PEI with 22-kDa) and Lipofectamine® LTX with PLUS™ despite the polyplex micelles do not equip specific endosomal escape functionality. This indicates that proper rod length regulation along with adequate ligand functionalization can compromise the absence of functionality of endosome escape.

Apart from the direction to augment the transfection capacity, which has shown to be successful in systemic application, a challenge to improve blood circulation should be demonstrated to achieve ideal formulation. To this end, a trade-off issue concerning the augmentation of PEG shielding and the concomitant elongation of the rod length has to be tackled. Thus, a block catiomer of PEG$_{20k}$-P(Asp(DET))$_{60}$-Chole was prepared. The conjugated cholesteryl group contributed to promote a number of binding block catiomers to pDNA beyond the charge stoichiometric ratio [47], which was ascribed to the adsorption of block catiomers onto the charge-neutralized polyplex by hydrophobic interaction, as evidenced by the binding profile corresponding the Freundlich

adsorption isotherm [49]. The incorporated cholesteryl groups in the polyplex core increased hydrophobicity of the core, driving the rod length shorter. Consequently, large number of PEG chains tethered on more compacted core surface of the polyplex micelles, giving augmented PEG crowding. Moreover, the rod length was limited to 76 nm, indicating the success of tackling the trade-off. It should be noted that the profile of the number of block catiomer binding with pDNA allowed for identifying the condition to obtain polyplex micelles without including free catiomers in solution but ensuring maximized polymer binding, i.e. N/P ratio of 4. The polyplex micelles prepared in this condition exhibited negligible toxicity both *in vitro* and *in vivo* and showed tumor-selective accumulation and antitumor efficacy by the cRGD attachment, thereby addressing both safety and efficiency issue [49]. It should be worth to note that a series of programmed functionalities are integrated in the proposed polyplex micelles along with satisfying structural requirements, high PEG crowding to escape MPS capture, core stabilization by conjugated hydrophobic group, ligand molecule for facilitating cellular uptake, catiomer for facilitating endosome escape, which is boosted by the attached cholesteryl group, rod length below the critical length for efficient cellular uptake, regularly folded pDNA for enhanced transcription, self-degradation profile of the P(Asp(DET)) catiomer for minimizing cytotoxicity, and moreover absence of free catiomer in polyplex solution. The cRGD-PEG$_{20k}$-P(Asp(DET))$_{60}$-Chole polyplex micelles exerted significant antitumor efficacy against pancreatic tumor mode by tumor vasculature targeting [49].

Besides of those systemic attempts, the attractive potency of long rod-shaped polyplex micelles, consisting of less folded pDNA, to elicit efficient transcription can be utilized once they are translocated in the cell. The trend that the lower the P(Lys) DP, the higher the efficiency was observed in cell-free gene expression system [23, 131] as well as in cellular gene expression after the cytosolic injection [34]. The same trend was observed *in vivo* by applying hydrodynamic injection target to skeletal muscle cells of mice from tail vain [132]. Note that this technique was originally reported for introducing naked pDNA into muscle cells; thus, it is likely that it allows direct intracellular translocation. It should be emphasized that polyplex micelles prepared from PEG$_{12k}$-*b*-P(Lys)$_{20}$ exhibited higher efficiency than the naked pDNA in these gene expression tests, most likely due to the synergistic effects of the increased nuclease tolerability and the transcription-favorable packaging. With this approach, significant antitumor effect over the naked pDNA was demonstrated against a distant pancreatic tumor by introducing sFlt-1 gene in skeletal muscle cells for systemically secreting [133], appealing great utility of this micelle formulation with this technique, called "protein factory" [132, 134]. Note that promoted *in vivo* gene expression was observed for long rod-shaped polyplex micelles prepared from PEG-*b*-PPA with following order; long rod shape > short rod shape > globular shape, after retrograde intrabiliary infusion to liver [40], which may be possible to assume the same aspect. In this way, the potency of the long rod-shaped polyplex micelles can be utilized *in vivo*, which may be applicable in other techniques skipping the cellular uptake process, such as gene gun, electroporation, and microbubbles.

## 1.5 Rod Shape or Toroid Shape

Other than rod and globular shape, toroid shape is often found in polyplex micelles (Figure 1.1) [24, 26–31, 40]. This shape is formed by spooling of pDNA and gains interest because of the analogy with the packaging scheme of virus genome [135–138]. The selective formation of toroid was previously demonstrated by complexing DNA with hexammine cobalt or spermidine, this toroid comprises multiple number of DNA after incorporating surrounding DNA molecules for growing [139, 140]. In contrast, in terms of structural analogy with virus, the toroid in polyplex micelles may be assumed to be more relevant regarding the single DNA packaging under the shell of PEG. However, the shape control of polyplex micelles had remained as a challenge. This subject has challenged by carefully modulating the interaction between pDNA and block catiomers by NaCl. It was demonstrated that pDNA was selectively folded into rod shape (95% in frequency) by complexing PEG-*b*-P(Asp(DET)) under the maximized interactive strength in the absence of NaCl; however, it was selectively spooled into toroid shape (90% in frequency) by complexation in the presence of 600 mM NaCl (Figure 1.4) [141]. It should be emphasized that the toroid polyplex micelles demonstrated superior transcription efficiency in cell-free evaluation; moreover, superior *in vivo* gene expression in the attempt
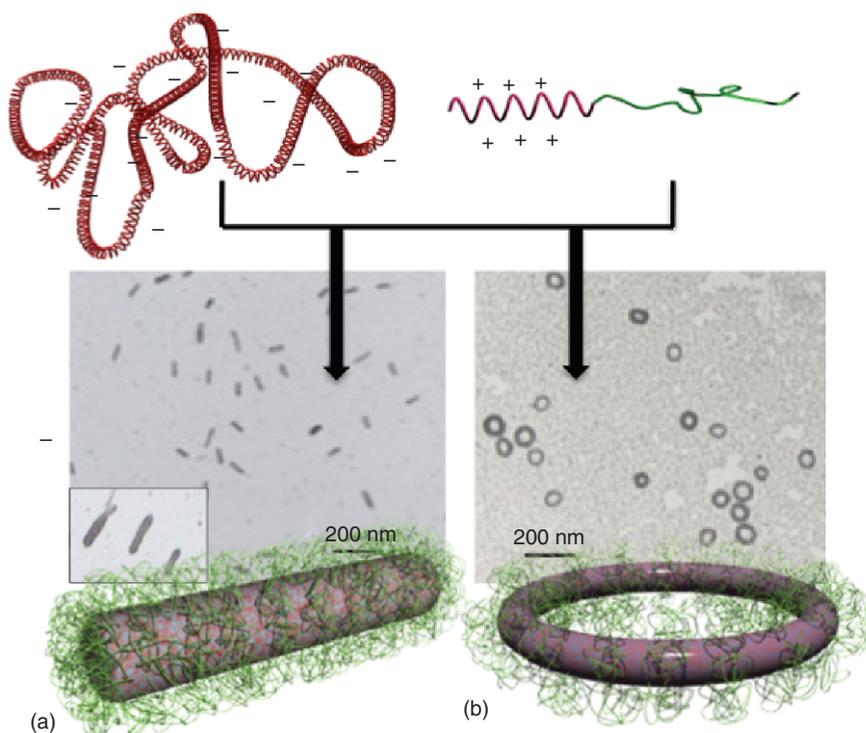


**Figure 1.4** Selective packaging of pDNA into (a) rod shape or (b) toroid shape by preparation at different NaCl concentration.

of the hydrodynamic application target to skeletal muscle cells as compared with rod-shaped polyplex micelles [141]. These biological features appeal the potential of the toroid-shaped polyplex micelles as "artificial viral vector." Of note, the NaCl concentration of 600 mM coincides with that of seawater, further making the toroid shape fascinating.

## 1.6 Summary

Molecular mechanism of DNA condensation by block catiomers was first highlighted to address the simple questions that how the long and rigid DNA can undergo condensation and form structural polymorphism. These studies provided ways to control pDNA packaging and thereby opportunities to find favorable, or unfavorable, structures for overcoming delivery process, identifying important issues to be managed for accommodating entire systemic delivery. Polyplex micelles prepared from strategically designed functional block catiomers, along with the controlled assembly with pDNA into suitable structure for the sake of addressing those issues, endowed self-driving functions to overcome entire systemic process. Further development of polyplex micelles along this molecular-technology-based direction will pave a way for safe and efficient nonviral gene therapy performed likewise virus.

## References

1 Minagawa, K., Matsuzawa, Y., Yoshikawa, K. et al. (1991). *FEBS Lett.* 295 (1–3): 67–69.

2 Bloomfield, V.A. (1997). *Biopolymers* 44 (3): 269–282.

3 Sergeyev, V.G., Pyshkina, O.A., Lezov, A.V. et al. (1999). *Langmuir* 9: 4434–4440.

4 Friedmann, T. and Roblin, R. (1972). *Science* 175 (4025): 949–955.

5 Behr, J.-P. (1994). *Bioconjugate Chem.* 5 (5): 382–389.

6 Mulligan, R.C. (1993). *Science* 260 (5110): 926–932.

7 Kabanov, A.V. and Kabanov, V.A. (1995). *Bioconjugate Chem.* 6 (1): 7–20.

8 Luo, D. and Saltzman, W.M. (2000). *Nat. Biotechnol.* 18 (1): 33–37.

9 Harada-Shiba, M., Takamisawa, I., Miyata, K. et al. (2009). *Mol. Ther.* 17 (7): 1180–1186.

10 Lee, M. and Kim, S.W. (2005). *Pharm. Res.* 22 (1): 1–10.

11 Ogris, M., Brunner, S., Schüller, S. et al. (1999). *Gene Ther.* 6 (4): 595–605.

12 Harada-Shiba, M., Yamauchi, K., Harada, A. et al. (2002). *Gene Ther.* 9 (6): 407–414.

13 Kataoka, K., Togawa, H., Harada, A. et al. (1996). *Macromolecules* 29 (26): 8556–8557.

14 Katayose, S. and Kataoka, K. (1997). *Bioconjugate Chem.* 8 (97): 702–707.

15 Cabral, H. and Kataoka, K. (2014). *J. Controlled Release* 190: 465–476.

16 Mochida, Y., Cabral, H., and Kataoka, K. (2017). *Expert Opin. Drug Delivery* 5247 (March): doi: 10.1080/17425247.2017.1307338.

**17** Lächelt, U. and Wagner, E. (2015). *Chem. Rev.* 150415062557000.

**18** Dash, P.R., Toncheva, V., Schacht, E., and Seymour, L.W. (1997). *J. Controlled Release* 48 (2–3): 269–276.

**19** Toncheva, V., Wolfert, M.A., Dash, P.R. et al. (1998). *Biochim. Biophys. Acta, Gen. Subj.* 1380 (3): 354–368.

**20** Mintzer, M.A. and Simanek, E.E. (2008). *Chem. Rev.* 109 (2): 259–302.

**21** Konstan, M.W., Davis, P.B., Wagener, J.S. et al. (2004). *Hum. Gene Ther.* 15 (12): 1255–1269.

**22** Davis, P.B. and Cooper, M.J. (2007). *AAPS J.* 9 (1): E11–E17.

**23** Takeda, K.M., Osada, K., Tockary, T.A. et al. (2016). *Biomacromolecules* 18: 36–43.

**24** Lam, J.K.W., Ma, Y., Armes, S.P. et al. (2004). *J. Controlled Release* 100 (2): 293–312.

**25** Oupický, D., Carlisle, R.C., and Seymour, L.W. (2001). *Gene Ther.* 8 (9): 713–724.

**26** Rackstraw, B.J., Martin, A.L., Stolnik, S. et al. (2001). *Langmuir* 17 (11): 3185–3193.

**27** Ziady, A.G., Gedeon, C.R., Miller, T. et al. (2003). *Mol. Ther.* 8 (6): 936–947.

**28** Osada, K., Yamasaki, Y., Katayose, S., and Kataoka, K. (2005). *Angew. Chem. Int. Ed.* 44 (23): 3544–3548.

**29** Boylan, N.J., Suk, J.S., Lai, S.K. et al. (2012). *J. Controlled Release* 157 (1): 72–79.

**30** Osawa, S., Osada, K., Hiki, S. et al. (2016). *Biomacromolecules* 17 (1): 354–361.

**31** Li, J., Chen, Q., Zha, Z. et al. (2015). *J. Controlled Release* 209: 77–87.

**32** Osada, K., Oshima, H., Kobayashi, D. et al. (2010). *J. Am. Chem. Soc.* 132 (35): 12343–12348.

**33** Ruff, Y., Moyer, T., Newcomb, C.J. et al. (2013). *J. Am. Chem. Soc.* 135 (16): 6211–6219.

**34** Osada, K., Shiotani, T., Tockary, T.A. et al. (2012). *Biomaterials* 33 (1): 325–332.

**35** Tockary, T.A., Osada, K., Chen, Q. et al. (2013). *Macromolecules* 46 (16): 6585–6592.

**36** Tockary, T.A., Osada, K., Motoda, Y. et al. (2016). *Small* 12 (9): 1193–1200.

**37** Chen, Q., Osada, K., Ishii, T. et al. (2012). *Biomaterials* 33 (18): 4722–4730.

**38** Qian, Y., Zha, Y., Feng, B. et al. (2013). *Biomaterials* 34 (8): 2117–2129.

**39** Rungsardthong, U., Deshpande, M., Bailey, L. et al. (2001). *J. Controlled Release* 73: 359–380.

**40** Jiang, X., Qu, W., Pan, D. et al. (2013). *Adv. Mater.* 25 (2): 227–232.

**41** Burke, R.S. and Pun, S.H. (2008). *Bioconjugate Chem.* 19 (3): 693–704.

**42** Ruponen, M. and Urtti, A. (1999). *Biochim. Biophys. Acta* 1415: 331–341.

**43** Miyata, K., Kakizawa, Y., Nishiyama, N. et al. (2004). *J. Am. Chem. Soc.* 126 (8): 2355–2361.

**44** Meng, F., Hennink, W.E., and Zhong, Z. (2009). *Biomaterials* 30 (12): 2180–2198.

**45** Talelli, M., Barz, M., Rijcken, C.J.F. et al. (2015). *Nano Today* 10 (1): 93–117.

**46** Naito, M., Ishii, T., Matsumoto, A. et al. (2012). *Angew. Chem. Int. Ed.* 51 (43): 10751–10755.

**47** Oba, M., Miyata, K., Osada, K. et al. (2011). *Biomaterials* 32 (2): 652–663.

**48** Ge, Z., Chen, Q., Osada, K. et al. (2014). *Biomaterials* 35 (10): 3416–3426.

**49** Chen, Q., Osada, K., Ge, Z. et al. (2016). *Biomaterials* 113: 253–265.

**50** Kizzire, K., Khargharia, S., and Rice, K.G. (2012). *Gene Ther.* 20 (4): 407–416.

**51** Kenausis, G.L., Vörös, J., Elbert, D.L. et al. (2000). *J. Phys. Chem. B* 104 (14): 3298–3309.

**52** Kim, W.J., Yockman, J.W., Jeong, J.H. et al. (2006). *J. Controlled Release* 114 (3): 381–388.

**53** Dash, P.R., Read, M.L., Barrett, L.B. et al. (1999). *Gene Ther.* 6 (4): 643–650.

**54** Kunath, K., Von Harpe, A., Petersen, H. et al. (2002). *Pharm. Res.* 19 (6): 810–817.

**55** Nomoto, T., Matsumoto, Y., Miyata, K. et al. (2011). *J. Controlled Release* 151 (2): 104–109.

**56** Takeda, K.M., Yamasaki, Y., Dirisala, A. et al. (2017). *Biomaterials* 126: 31–38.

**57** Oba, M., Vachutinsky, Y., Miyata, K. et al. (2010). *Mol. Pharmaceutics* 7 (2): 501–509.

**58** Vachutinsky, Y., Oba, M., Miyata, K. et al. (2011). *J. Controlled Release* 149 (1): 51–57.

**59** Dirisala, A., Osada, K., Chen, Q. et al. (2014). *Biomaterials* 35 (20): 5359–5368.

**60** Klutz, K., Schaffert, D., Willhauck, M.J. et al. (2011). *Mol. Ther.* 19 (4): 676–685.

**61** Wagner, E., Curiel, D., and Cotten, M. (1994). *Adv. Drug Delivery Rev.* 14 (1): 113–135.

**62** Wickham, T.J. (2003). *Nat. Med.* 9 (1): 135–139.

**63** Wagner, E. (1998). *J. Controlled Release* 53 (1–3): 155–158.

**64** Futaki, S. (2005). *Adv. Drug Delivery Rev.* 57 (4): 547–558.

**65** Nakase, I., Takeuchi, T., Tanaka, G., and Futaki, S. (2008). *Adv. Drug Delivery Rev.* 60 (4–5): 598–607.

**66** Bolhassani, A. (2011). *Biochim. Biophys. Acta, Rev. Cancer* 1816 (2): 232–246.

**67** Sawant, R. and Torchilin, V. (2010). *Mol. Biosyst.* 6 (4): 628–640.

**68** Gupta, B., Levchenko, T.S., and Torchilin, V.P. (2005). *Adv. Drug Delivery Rev.* 57 (4): 637–651.

**69** Miura, Y., Takenaka, T., Toh, K. et al. (2013). *ACS Nano* 7 (10): 8583–8592.

**70** Ishii, T., Miyata, K., Anraku, Y. et al. (2016). *Chem. Commun.* 52 (7): 1517–1519.

**71** Brülisauer, L., Kathriner, N., Prenrecaj, M. et al. (2012). *Angew. Chem. Int. Ed.* 51 (50): 12454–12458.

**72** Takae, S., Miyata, K., Oba, M. et al. (2008). *J. Am. Chem. Soc.* 130 (18): 6001–6009.

**73** Ping, Y., Hu, Q., Tang, G., and Li, J. (2013). *Biomaterials* 34 (27): 6482–6494.

**74** Zhu, C., Zheng, M., Meng, F. et al. (2012). *Biomacromolecules* 13 (3): 769–778.

**75** Wei, H., Volpatti, L.R., Sellers, D.L. et al. (2013). *Angew. Chem. Int. Ed.* 52 (20): 5377–5381.

**76** Hatakeyama, H., Akita, H., Ito, E. et al. (2011). *Biomaterials* 32 (18): 4306–4316.

**77** Huang, S., Shao, K., Kuang, Y. et al. (2013). *Biomaterials* 34 (21): 5294–5302.

**78** Champion, J.A., Katare, Y.K., and Mitragotri, S. (2007). *J. Controlled Release* 121 (1–2): 3–9.

**79** Geng, Y., Dalhaimer, P., Cai, S. et al. (2007). *Nat. Nanotechnol.* 2 (4): 249–255.

**80** Champion, J.A. and Mitragotri, S. (2009). *Pharm. Res.* 26 (1): 244–249.

**81** Zhang, K., Fang, H., Chen, Z. et al. (2008). *Bioconjug. Chem.* 19: 1880–1887.

**82** Lim, J.P. and Gleeson, P.A. (2011). *Immunol. Cell Biol.* 89 (8): 836–843.

**83** Mcmahon, H.T. and Boucrot, E. (2011). *Nat. Rev. Mol. Cell Biol.* 12 (8): 517–533.

**84** Rejman, J., Oberle, V., Zuhorn, I.S., and Hoekstra, D. (2004). *Biochem. J* 377 (Pt 1): 159–169.

**85** Pelkmans, L. and Helenius, A. (2002). *Traffic* 3 (13): 311–320.

**86** Conner, S.D. and Schmid, S.L. (2003). *Nature* 422 (6927): 37–44.

**87** Behr, J. (1997). *Chim. Int. J. Chem.* 2 (1): 34–36.

**88** Boussif, O., Lezoualc'h, F., Zanta, M.A. et al. (1995). *Proc. Natl. Acad. Sci. U.S.A.* 92 (16): 7297–7301.

**89** Yang, S. and May, S. (2008). *J. Chem. Phys.* 129 (18): 1–9.

**90** Midoux, P. and Monsigny, M. (1999). *Bioconjugate Chem.* 10: 406–411.

**91** Hwang, H.S., Hu, J., Na, K., and Bae, Y.H. (2014). *Biomacromolecules* 15: 3577–3586.

**92** Leng, Q. and Mixson, A.J. (2005). *Nucleic Acids Res.* 33 (4): 1–9.

**93** Wong, S.Y., Sood, N., and Putnam, D. (2009). *Mol. Ther.* 17 (3): 480–490.

**94** Haensler, J. and Szoka, F.C. (1993). *Bioconjugate Chem.* 4 (5): 372–379.

**95** Kukowska-Latallo, J.F., Bielinska, A.U., Johnson, J. et al. (1996). *Proc. Natl. Acad. Sci. U.S.A.* 93 (10): 4897–4902.

**96** Arima, H., Kihara, F., Hirayama, F., and Uekama, K. (2001). *Bioconjugate Chem.* 12 (4): 476–484.

**97** Uchida, H., Miyata, K., Oba, M. et al. (2011). *J. Am. Chem. Soc.* 133 (39): 15524–15532.

**98** Miyata, K., Oba, M., Nakanishi, M. et al. (2008). *J. Am. Chem. Soc.* 130 (48): 16287–16294.

**99** Benjaminsen, R.V., Mattebjerg, M.A., Henriksen, J.R. et al. (2012). *Mol. Ther.* 21 (1): 149–157.

**100** Miyata, K., Nishiyama, N., and Kataoka, K. (2012). *Chem. Soc. Rev.* 41 (7): 2562.

**101** Wagner, E. (2012). *Acc. Chem. Res.* 45 (7): 1005–1013.

**102** Nakanishi, M., Park, J.S., Jang, W.D. et al. (2007). *React. Funct. Polym.* 67 (11 SPEC. ISS): 1361–1372.

**103** Martin, I., Dohmen, C., Mas-Moruno, C. et al. (2012). *Org. Biomol. Chem.* 10 (16): 3258.

**104** Plank, C., Zauner, W., and Wagner, E. (1998). *Adv. Drug Delivery Rev.* 34 (1): 21–35.

**105** Wagner, E., Plank, C., Zatloukal, K. et al. (1992). *Proc. Natl. Acad. Sci. U.S.A.* 89 (17): 7934–7938.

**106** Oba, M., Aoyagi, K., Miyata, K. et al. (2008). *Mol. Pharmaceutics* 5 (6): 1080–1092.

**107** Christie, R.J., Matsumoto, Y., Miyata, K. et al. (2012). *ACS Nano* 6 (6): 5174–5189.

**108** Berg, K., Selbo, P.K., Prasmickaite, L. et al. (1999). *Cancer Res.* 59 (6): 1180–1183.

**109** Høgset, A., Prasmickaite, L., Tjelle, T.E., and Berg, K. (2000). *Hum. Gene Ther.* 11 (6): 869–880.

**110** Høgset, A., Prasmickaite, L., Selbo, P.K. et al. (2004). *Adv. Drug Delivery Rev.* 56 (1): 95–115.

**111** Nishiyama, N., Stapert, H.R., Zhang, G.D. et al. (2003). *Bioconjugate Chem.* 14 (1): 58–66.

**112** Jang, W.D., Nishiyama, N., Zhang, G.D. et al. (2005). *Angew. Chem. Int. Ed.* 44 (3): 419–423.

**113** Nishiyama, N., Iriyama, A., Jang, W.-D. et al. (2005). *Nat. Mater.* 4 (12): 934–941.

**114** Nomoto, T., Fukushima, S., Kumagai, M. et al. (2014). *Nat. Commun.* 5: 3545.

**115** Grosse, S., Thevenot, G., Monsigny, M., and Fajac, I.W. (2006). *J. Gene Med.* 8: 845–851.

**116** Grandinetti, G. and Reineke, T.M. (2012). *Mol. Pharmaceutics* 9 (8): 2256–2267.

**117** Dworetzky, S.I., Lanford, R.E., and Feldherr, C.M. (1988). *J. Cell Biol.* 107 (4): 1279–1287.

**118** Pante, N. and Kann, M. (2002). *Mol. Biol. Cell* 13 (2): 425–434.

**119** Escriou, V., Carrière, M., Scherman, D., and Wils, P. (2003). *Adv. Drug Delivery Rev.* 55 (2): 295–306.

**120** Zabner, J., Fasbender, A.J., Moninger, T. et al. (1995). *J. Biol. Chem.* 270: 18997–19007.

**121** Pollard, H., Remy, J.S., Loussouarn, G. et al. (1998). *J. Biol. Chem.* 273 (13): 7507–7511.

**122** Schaffer, D.V., Fidelman, N.A., Dan, N., and Lauffenburger, D.A. (2000). *Biotechnol. Bioeng.* 67 (5): 598–606.

**123** Honoré, I., Grosse, S., Frison, N. et al. (2005). *J. Controlled Release* 107 (3): 537–546.

**124** Bieber, T., Meissner, W., Kostin, S. et al. (2002). *J. Controlled Release* 82: 441–454.

**125** Cornelis, S., Vandenbranden, M., Ruysschaert, J.-M., and Elouahabi, A. (2002). *DNA Cell Biol.* 21 (2): 91–97.

**126** Matsumoto, Y., Itaka, K., Yamasoba, T., and Kataoka, K. (2009). *J. Gene Med.* 11: 615–623.

**127** Itaka, K., Ishii, T., Hasegawa, Y., and Kataoka, K. (2010). *Biomaterials* 31 (13): 3707–3714.

**128** Furugaki, K., Cui, L., Kunisawa, Y. et al. (2014). *PLoS One* 9 (7): e101854.

**129** Cui, L., Osada, K., Imaizumi, A. et al. (2015). *J. Controlled Release* 206: 220–231.

**130** Miyata, K., Oba, M., Kano, M.R. et al. (2008). *Pharm. Res.* 25 (12): 2924–2936.

**131** Aono, R., Yuba, E., Harada, A., and Kono, K. (2014). *ACS Macro Lett.* 3: 333–336.

**132** Hagstrom, J.E., Hegge, J., Zhang, G. et al. (2004). *Mol. Ther.* 10 (2): 386–398.

**133** Itaka, K., Osada, K., Morii, K. et al. (2010). *J. Controlled Release* 143 (1): 112–119.

**134** Lu, Q.L., Bou-Gharios, G., and Partridge, T.A. (2003). *Gene Ther.* 10 (2): 131–142.

**135** Golan, R., Pietrasanta, L.I., Hsieh, W., and Hansma, H.G. (1999). *Biochemistry* 38 (42): 14069–14076.

**136** Hud, N.V. and Vilfan, I.D. (2005). *Annu. Rev. Biophys. Biomol. Struct.* 34: 295–318.

**137** Cerritelli, M.E., Cheng, N., Rosenberg, A.H. et al. (1997). *Cell* 91 (2): 271–280.

**138** Leforestier, A. and Livolant, F. (2009). *Proc. Natl. Acad. Sci. U.S.A.* 106 (23): 9157–9162.

**139** Vilfan, I.D., Conwell, C.C., Sarkar, T., and Hud, N.V. (2006). *Biochemistry* 45 (26): 8174–8183.

**140** Sarkar, T., Vitoc, I., Mukerji, I., and Hud, N.V. (2007). *Nucleic Acids Res.* 35 (3): 951–961.

**141** Li, Y., Osada, K., Chen, Q. et al. (2015). *Biomacromolecules* 16 (9): 2664–2671.